10

Optical and laser performance of Yb:YSAG ceramics

© V.Yu. Zmykhov[1], D.A. Guryev[1], V.S. Tsvetkov[1], E.A. Dobretsova[1], Yu.N. Pyrkov[1], S.V. Kuznetsov[1], M.S. Nikova[2], V.A. Tarala[2], D.S. Vakalov[2], A.A. Kravtsov[2], V.B. Tsvetkov[1]

[1] Prokhorov General Physics Institute of the Russian Academy of Sciences, 119991 Moscow, Russia
[2] North-Caucasus Federal University,

e-mail: Vadimzhmykhov56@gmail.com

Received November 02, 2022
Revised December 21, 2022
Accepted April 09, 2023

8.3(3) at.% Yb:YSAG ceramics ($Y_{2.55}Yb_{0.25}Sc_{1.00}Al_{4.2}O_{12}$) have been prepared via solid solution powder sintering. The optical and lasing characteristics have been successfully studied. Lasing was obtained on the basis of Yb:YSAG ceramics and the characteristics of laser radiation were studied at different transmittances of the output mirror of the resonator. The maximum lasing power was 1.8 W at 3.6 W of absorbed pumping in the quasi-cw generation mode. The maximum differential efficiency was 57% for a mirror with a transmittance of 14.5%.

Keywords: Optical ceramics, ytterbium, luminescence, laser generation, radiative lifetimes, rare-earth elements, lasing output power.

DOI: 10.61011/EOS.2023.05.56506.68-22

Introduction

The development of laser oxide and fluoride ceramics is a serious challenge of optical materials science at the present stage. Optical ceramics based on yttrium-aluminum garnet and other materials doped with rare-earth ions has been widely recognized as a promising replacement for single-crystal active media [1] as well as in magneto-optical devices [2,3]. This became possible due to its significant advantages such as the opportunity of achieving a high concentration of active ions and high doping homogeneity [4], the opportunity of manufacturing samples with a large aperture and realizing multilayer structures [5]. In recent years, optical ceramics and crystals with a garnet structure based on yttrium, aluminum, and scandium oxides doped with rare-earth ions have been of great interest as active media for solid-state lasers [6–9]. One of the ground factors determining the quality of optical ceramics is the exclusion of impurity phases in the initial ceramic powders, since they lead to the appearance of scattering centers and significantly reduce the transmission coefficient of ceramics [9]. One of the significant advantages is the opportunity of implementing a multilayer structure, since this allows for multifunctionality and optimization of the properties of the optical medium. For example, more efficient thermal control during laser operation can be achieved by controlling the concentration of doping ions of rare earth elements in the initial materials (for example, longitudinal temperature and mechanical stress gradients in solid-state lasers with end-pumped diode lasers can be minimized) [10].

An alternative to Nd^{3+}-containing media for obtaining lasing in the region around $1\,\mu$m are materials doped with Yb^{3+} ions. Ytterbium active media have a smaller quantum generation defect compared to neodymium media, and also have a wider emission band. Because of this, matrices doped with ytterbium are more promising for use as active media in femtosecond lasers. Yb^{3+} ions (electronic configuration $4f^{13}$) have one excited state $^2F_{5/2}$ with an energy of approximately $10200-11100\,cm^{-1}$, which is well suited for use as pump sources for commercially available InGaAs laser diodes emitting in the region of $915-980$ nm. The level structure of the Yb^{3+} ions excludes absorption from the $^2F_{5/2}$ excited state, since there are no higher levels in the Yb^{3+} ion.

The aim of this paper was to study the spectral-lasing characteristics of 8.3(3) at.% Yb:YSAG ($Y_{2.55}Yb_{0.25}Sc_{1.00}Al_{4.2}O_{12}$) ceramics depending on the transmittance of the resonant cavity output mirror.

Ceramics manufacturing

Ceramic powders were synthesized by the modified reverse coprecipitation method [11–12]. Ammonium hydroxide (25%, extra pure, Sigma Tech), $AlCl_3{\cdot}6H_2O$ (99%, Acros Organics), $YCl_3{\cdot}6H_2O$ (99.9%, Chemical Point), $YbCl_3{\cdot}6H_2O$ (99,9%, Chemical Point), $ScCl_3{\cdot}6H_2O$ (99.9%, Novosibirsk Rare Earth Plant) were used as initial reagents, $(NH_4)_2SO_4$ was a dispersant (99%, Stavreakhim), $MgCl_2{\cdot}6H_2O$ was a magnesium sintering agent (99%, Interchem), ethanol (95%, Fereyn) was a solvent. All reagents were used without further purification. Deionized water was used for all operations, including laboratory glassware washing.

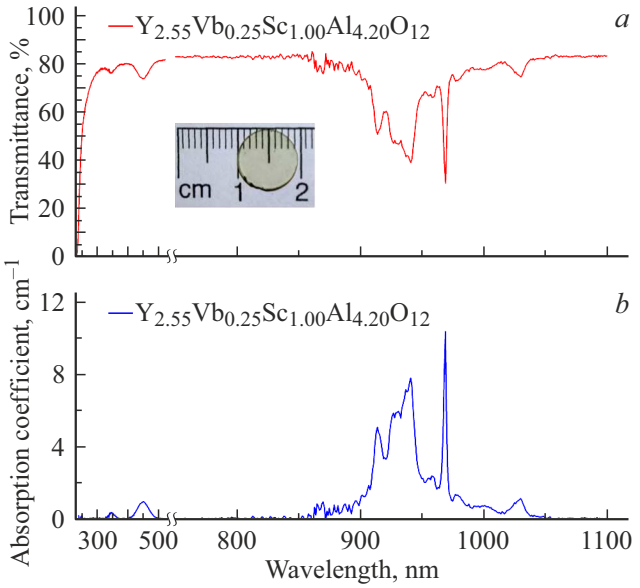

Figure 1. Transmittance spectrum (a) and absorption coefficient (b) of 8.3(3) at.% Yb:YSAG transparent ceramics. The insert shows an image of the ceramic sample.

$Y_{2.55}Yb_{0.25}Sc_{1.00}Al_{4.2}O_{12}$ composition was selected from the area of existence of single-phase solid solutions based on yttrium-scandium-aluminum garnets doped with ytterbium according to [13]. The scandium ion can occupy both dodecahedral and octahedral positions of the garnet crystal lattice due to the closeness of the radii of the cations of yttrium and scandium, scandium and aluminum [14], which is confirmed by data both on the growth of the corresponding single crystals [15,16], and on obtaining optical ceramics [17].

The $Y_{2.55}Yb_{0.25}Sc_{1.00}Al_{4.2}O_{12}$ ceramic sample was made in the form of a disk 10 mm in diameter and 1 mm thick. An image of the $Y_{2.55}Yb_{0.25}Sc_{1.00}Al_{4.2}O_{12}$ ceramics is shown in the insert to Fig. 1.

Absorption and luminescence spectra

The transmittance spectrum of Yb:YSAG ceramics in the range from 200 to 1800 nm was measured with a spectral resolution of 0.5 nm on the Shimadzu UV-3101PC spectrophotometer at room temperature (Fig. 1,a) . The transmission spectrum in the range of 970–1070 nm (electronic transitions $^2F_{7/2} \rightarrow {}^2F_{5/2}$) of the Yb^{3+} ion was measured with a spectral resolution of 0.1 nm. The intensity of the transmitted light can be described by the expression

$$I = I_0(1 - R_\Sigma)\exp\left[-(\alpha_{\text{scat}} + \alpha_{\text{abs}})l\right], \qquad (1)$$

where I and I_0 are intensities of a plane monochromatic wave of radiation incident and passing through a layer of matter, respectively, $R_\Sigma = \left(\frac{2R_1}{1+R_1}\right)$ is a reflection loss from two sample surfaces, taking into account multiple reflection in the sample in the absence of interference (R_1 is a is a reflection coefficient from the sample-air interface), α_{scat} is a scattering loss coefficient, α_{abs} is an absorption factor, and l is a sample length. Then the transmittance spectrum was adjusted to 100%, and then the attenuation coefficient (loss factor) was calculated as $\alpha = \alpha_{\text{abs}} + \alpha_{\text{scat}}$ by the formula

$$I = I_0 e^{-al}. \qquad (2)$$

In the wavelength range of 500–1800 nm, the transmittance of transparent Yb:YSAG ceramics with 8.3(3) at.% ytterbium corresponds to the value for a single crystal of yttrium-aluminum garnet (10 at.% Yb^{3+}:$Y_3Al_5O_{12}$) of high optical quality [18,19].

The availability of the absorption bands in the short-wave region of the spectrum (300–500 nm) is caused by the partial reduction of Yb^{3+} for Yb^{2+} [20], as well as the presence of oxygen vacancies [21], the concentrations of which can be reduced after annealing in air [22,23].

Practically in the entire spectral range under study, a transmittance of more than 80% is retained, which indicates the high quality of the ceramics. At wavelengths less than 500 nm, a decrease in the transmittance is observed, indicating the existence of a few optical scattering centers associated with microporosity [24,25]. Since the sample does not contain secondary phases [26], two sources of scattering are possible: changes in the refraction index at grain boundaries and porosity. Since the refraction index of YSAG is about 1.83, the effect of porosity on optical scattering will be much greater than the effect of grain boundaries [27,28]. In this connection, microporosity in the pore size range of the order of the wavelength of light is the main source of scattering. Low optical loss due to scattering can provide high laser performance of 8.3(3) at.% Yb:YSAG transparent ceramics.

The luminescence spectra of the Yb:YSAG ceramics at $T = 300$ K and $T = 77$ K in the range of 970–1070 nm were recorded on the ARC SpectraPro-300i monochromator using an InGaAs detector with thermoelectric cooling under excitation by a diode laser at a wavelength of 972 nm. The spectral resolution was 0.3 nm and 1.4 nm at 77 and 300 K, respectively (Fig. 2).

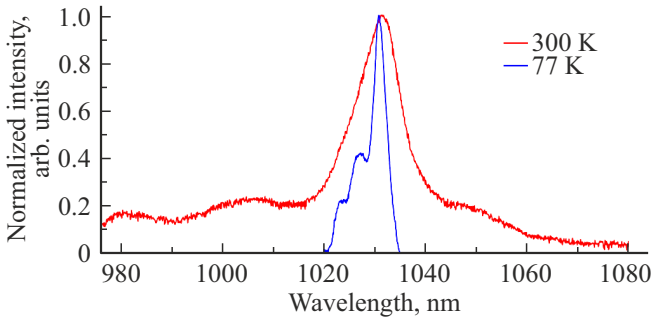

Figure 2. Luminescence spectra of 8.3(3) at.% Yb:YSAG optical ceramics in the $^2F_{5/2} \rightarrow {}^2F_{7/2}$ transition in the Yb^{3+} ion being measured at $T = 300$ K (red line) and $T = 77$ K (blue line).

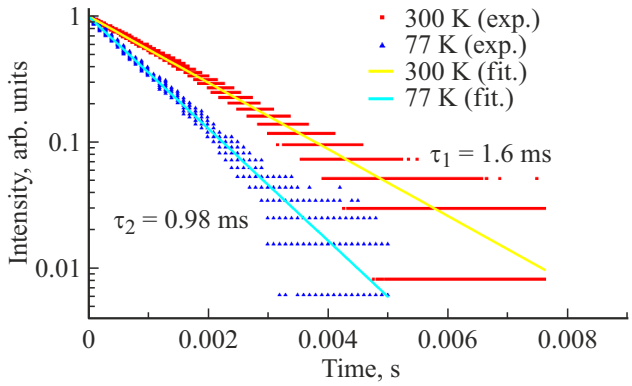

Figure 3. Luminescence decay kinetics of the $^2F_{5/2}$ multiplet for 8.3(3) at.% Yb : YSAG ceramics being measured at $T = 300$ K and $T = 77$ K.

The emission peak of 1031.3 nm does not shift at decreasing of temperature from 300 to 77 K. But we observe broadening of the luminescence line with a change in temperature that is caused by the electron-phonon interaction The wide range of emission wavelengths can be useful for generating short pulses in the mode-locking regime. To obtain more reliable information on the prospects for the use of materials, we calculated the radiation cross section using the Fuchtbauer – Ladenburg formula [29]. The maximum value of the radiation cross section was $1.126 \cdot 10^{-20}$ cm^2.

The experimental luminescence decay time at the $^2F_{5/2} \rightarrow {}^2F_{7/2}$ transition in Yb:YSAG ceramics was recorded using the MDR-12 monochromator (SOL Instruments). A diode laser (ATC.Semiconductor devices LDD-10) with a radiation wavelength of 972 nm was used as an excitation source The signal was recorded using the FD10-GA detector. The duration of the luminescence excitation pulse during the registration of luminescence decay curves was 20 ms, the duration of the front/decay pulse was less than 1 μs. The luminescence kinetics is usually measured by excitation with a short (significantly shorter than the lifetime) light pulse. However, in case of using a diode laser as an excitation source, this is impossible due to the low energy of the pulse, so we used a sufficiently long excitation pulse (to accumulate a significant number of excited ytterbium ions) with a short trailing edge. In this case, the lifetime measurement accuracy is determined only by the ratio of the duration of the trailing edge (decay) of the exciting pulse and the luminescence lifetime; the duration of the pulse top can only affect the magnitude of the luminescence signal.

Based on the luminescence decay kinetics being measured at $T = 300$ K and $T = 77$ K, the fluorescence lifetimes were estimated to be 1.6 and 0.98 ms, respectively (Fig. 3).

The $^2F_{5/2}$ decay curves are described by a single-exponential model, which may indicate the presence of one only optical center of active ions. The lifetime of ytterbium ions being recorded at 77 K is close to the lifetime of ytterbium ions in the YAG crystal (0.95 ms). The increase of the fluorescence decay time observed at room temperature may be the result of the interaction of excited Yb^{3+} ions, an increase in the reabsorption effect due to the overlap of the luminescence and absorption spectra increasing with temperature, or a lower transition probability characteristic of higher-lying Stark sublevels that are connected with increasing temperature. It is difficult to establish the exact reason for the change in the lifetime of the $^2F_{5/2}$ level of Yb^{3+} ions at this stage. These alleged causes have been described in [30–32].

Table 1. Quasi-continuous wave lasing characteristics

T_{oc}	Differ. Efficiency	Efficiency	Max. power, W
HR	3.4 ± 0.1%	2.8 ± 0.1%	0.10 ± 0.01
5%	36.0 ± 0.4%	31.8 ± 1.4%	1.15 ± 0.04
10%	48.0 ± 1.0%	43.4 ± 1.9%	1.57 ± 0.05
14.5%	57.0 ± 0.6%	50.0 ± 2.2%	1.81 ± 0.05

Continuous wave and quasi-continuous wave lasing

The study of the lasing characteristics of Yb:YSAG ceramics was carried out on a stand, the layout of which is shown in Fig. 4.

For cooling, the ceramic sample was fixed in a holder made of aluminum plates. Indium foil was used as an interface between the sample and the plates. The laser cavity was formed by two spherical mirrors. Input coupler of the laser cavity was highly reflective ($R > 99.5\%$) at the lasing wavelength (≈ 1030 nm) and had a radius of curvature $R = 100$ mm. Spherical mirrors with curvature radius $R = 50$ mm with different transmittances T_{oc} (0.5, 5.5, 10.0, and 14.5%) at the lasing wavelength were used as the output coupler. The distance between the mirrors was 2 cm. Ceramics was placed at a distance of 5 mm from the input mirror. To pump the Yb:YSAG ceramics, we used a laser diode with a fiber output of radiation with a wavelength of 938 nm and a fiber core diameter of 105 μm. The pumping radiation was focused using a system of two lenses (L1 and L2 in Fig. 4). The pumping spot diameter in the active element was approximately 100 μm. The laser cavity and pumping system were chosen in such a way to maximize the overlap of the pumping and generation areas to produce efficient single transverse mode operation.

Lasing characteristics of the ceramics were studied using output couplers with different transmittances at the lasing wavelength. The studies were carried out in two pumping regimes: continuous wave and quasi-continuous wave. In the case of quasi-continuous pumping, the duration of

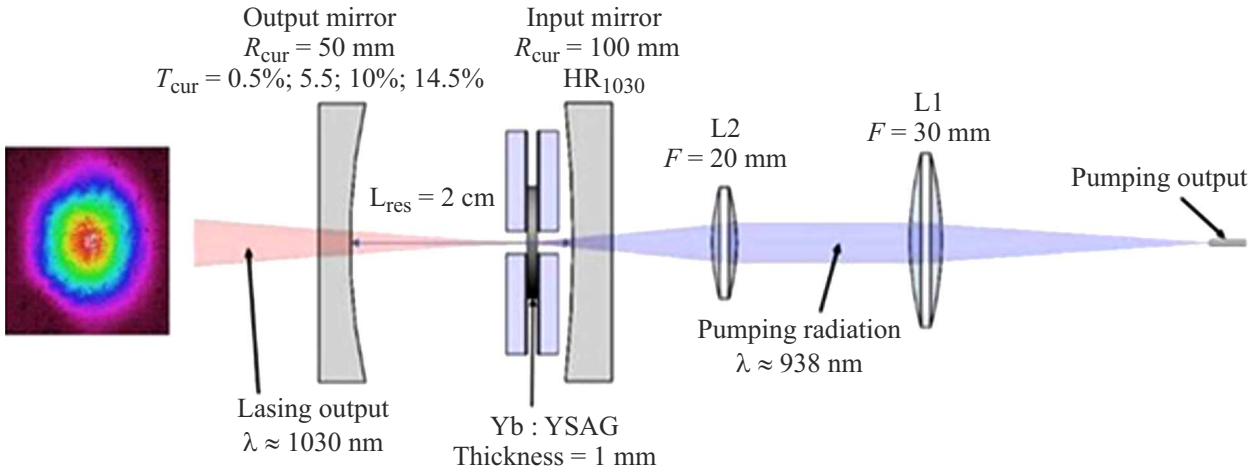

Figure 4. Diagram of pumping system and resonant cavity of a Yb:YSAG laser.

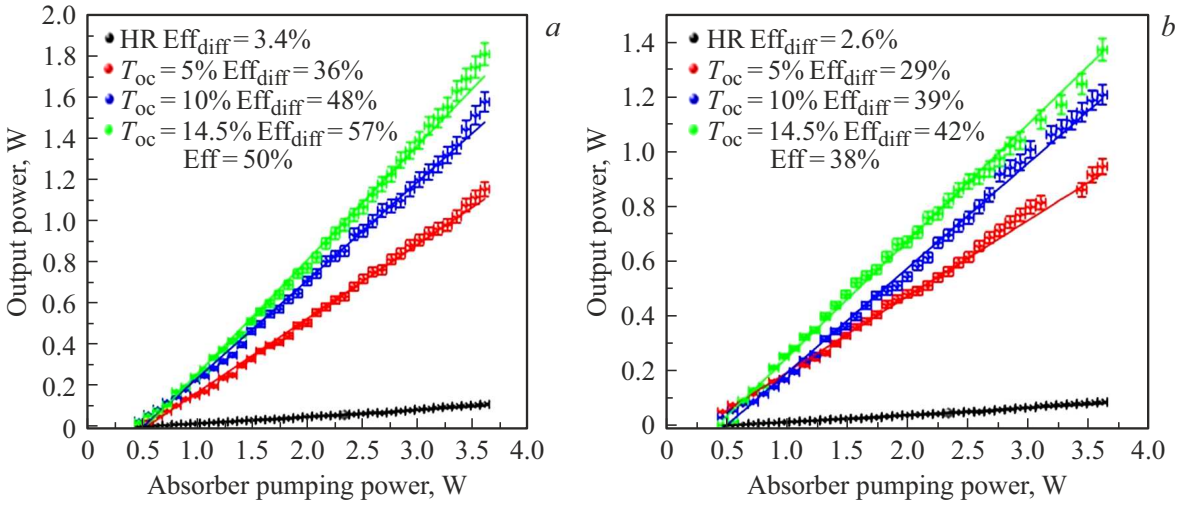

Figure 5. Dependences of the output power of a laser based on Yb:YSAG ceramics at different transmittances of the output coupler: *a* — for quasi-continuous wave lasing, *b* — for continuous wave lasing.

Table 2. Continuous wave lasing characteristics

T_{oc}	Differ. Efficiency	Efficiency	Max. power, W
HR	2.6 ± 0.1%	2.5 ± 0.1%	0.09 ± 0.03
5%	28.9 ± 0.3%	26.1 ± 1.9%	0.94 ± 0.03
10%	39.0 ± 1.9%	33.5 ± 1.5%	1.20 ± 0.04
14.5%	41.7 ± 1.9%	37.9 ± 1.7%	1.37 ± 0.04

the pumping pulses was 3 ms, and the pulse repetition frequency was 30 Hz.

Dependences of the output power of a laser based on Yb:YSAG ceramics at different transmittances of the output couplers are shown in Fig. 5. The maximum output power was obtained using an output coupler with a transmittance coefficient at the lasing wavelength of 14.5% and amounted to 1.80±0.05 W at an absorbed pumping power of 3.60 ± 0.12 W. The slope efficiency was 57.00 ± 0.61%. In the continuous wave pumping regime, the maximum power was 1.37 ± 0.04W with a slope efficiency of 41.70 ± 1.91%. Table 1 and Table 2 show the values of the laser efficiency and the maximum values of the output power being obtained using different output couplers.

A significant difference between the lasing characteristics in the quasi-continuous wave and continuous wave pumping regimes lies in the fact that the negative effect of thermooptical effects on the lasing characteristics is stronger in the cw pump mode than in the quasi-continuous wave pumping regime.

For all mirrors, the degree of radiation polarization was studied using the Glan prism. In all cases, it was determined that the lasing radiation was linearly polarized. The results of studying the radiation polarization for a

Table 3. Comparison of laser characteristics of ceramics

Work	Ceramics	Maximum output power in quasi-continouos wave regime, W	Slope efficiency, %	Efficiency, %	Transmittance of the output coupler, %
[33]	10 at.% Yb:$Y_3ScAl_4O_{12}$	9.2	58.7	54.1	18.8
[34]	15 at.% Yb:$Y_3ScAl_4O_{12}$	1.12	54	46	20
[35]	10 at.% Yb:$Y_3Sc_{1,5}Al_{3,5}O_{12}$	6.3	67.8	-	18.8
[35]	5 at.% Yb:$Y_3ScAl_4O_{12}$	10.12	58.1	53.8	18.8
[36]	10 at.% Yb:$Y_3Sc_{1.5}Al_{3.5}O_{12}$	10.8	66.4	62.8	18.8
[36]	10 at.% Yb : YAG	-	71.6	66.3	18.8
This study	8.3(3) at.%$Y_{2.55}Yb_{0.25}Sc_{1.00}Al_{4.2}O_{12}$	1.8	57	50	14.5

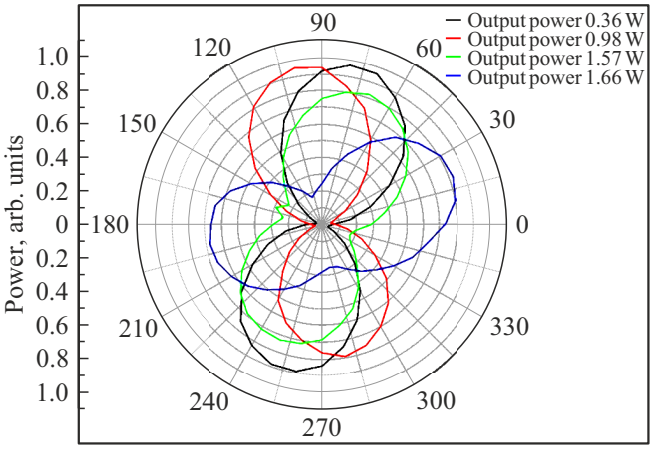

Figure 6. Polarization characteristics of laser radiation. Color indicates data at different lasing powers: black — at 0.63 W, red — at 0.98 W, green — at 1.57 W, blue — at 1.66 W.

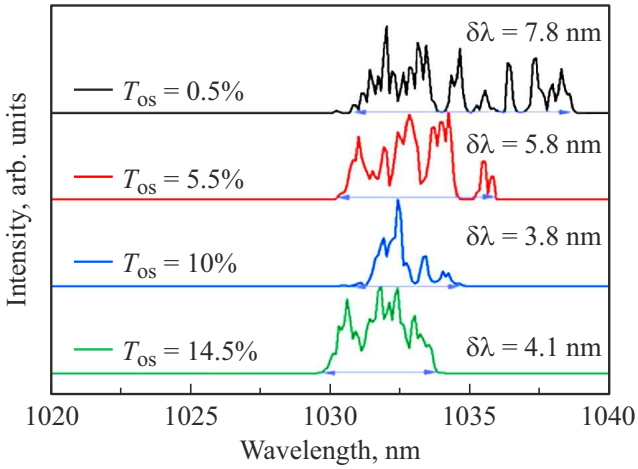

Figure 7. Spectra of laser radiation measured at an absorbed pumping power of 2.4 W.

mirror with $T_{oc} = 10\%$ for different levels of laser output power in the quasi-continuous mode are shown in Fig. 6. The effect of laser radiation polarization with the use of an optically isotropic medium is rather unexpected, as is the observed rotation of the laser radiation polarization plane with increasing pumping power. Perhaps this is a consequence of the thermomechanical stresses induced in the active medium. This effect is under study now.

The spectral characteristics of laser radiation are shown in Fig. 7. The lasing spectrum of the ceramics depended on the transmittance of the output mirror. A decrease in the transmittance led to a broadening of the lasing spectrum due to the fact that for mirrors with a lower transmittance the lasing losses were smaller; therefore, the lasing threshold for the edges of the amplification spectrum also became smaller. It should also be noted that the spectrum was broadened only to the long wavelength area. This is due to the fact that in the wavelength range < 1030 nm, the signal amplification did not exceed the losses caused by the absorption of lasing radiation associated with the overlap of the absorption and luminescence spectra of Yb^{3+} ions.

An increase in output generation characteristics can be achieved by applying antireflection coatings on ceramics on both sides.

The obtained results were compared with the lasing characteristics of similar ceramics (Table 3) [33–36]. The values of the slope efficiency and lasing efficiency achieved in this paper were comparable with the literature data, while the maximum transmittance of the output mirror was lower than in the above-mentioned works.

Intracavity losses play an important role in laser system optimization, especially in Q-switching [38]. Findlay–Clay analysis [39,40] uses the relationship between losses and threshold gain to determine the amount of loss in the active medium:

$$-\ln R = 2g_0 l - \delta, \qquad (3)$$

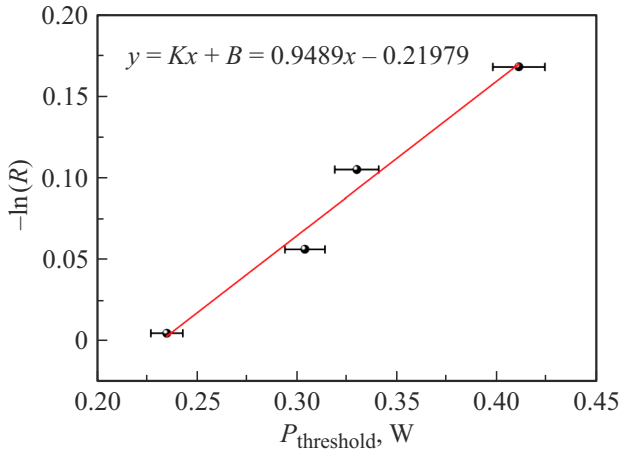

Figure 8. The dependence of the natural logarithm of the output couplers reflectance on the threshold power of the pumping radiation.

Table 4. Minimum values of the pumping power and the natural logarithm of the reflectance of the output coupler

Reflectance of the output coupler	Threshold pumping power, W	-ln$R$
0.995	0.235 ± 0.008	0.00501
0.945	0.304 ± 0.009	0.05650
0.900	0.330 ± 0.011	0.10536
0.845	0.411 ± 0.013	0.16842

where R — reflectance of the output mirror, g_0 — amplification coefficient, δ — non-radiative losses in the resonant cavity.

The threshold values of the pumping power and the natural logarithm of the reflectance of the output coupler are given in Table 4.

The dependence of the natural logarithm of the output couplers reflectance on the threshold power of the pumping radiation is shown in Fig. 8. The resulting curve was approximated by a linear dependence

$$y = Kx + B, \quad (4)$$

where K — coefficient of proportionality related to the amplification coefficient, B — lasing radiation losses in the resonant cavity per double bypass.

Calculation according to Findley.Clay method shows that the intracavity losses of the lasing radiation were about 0.22 (22%) per round trip of the cavity This value corresponds to the total losses of lasing radiation in the entire resonator. However, it should be noted that the largest contribution to the resonator losses is made by the active element, the losses of which are the sum of scattering by defects, absorption of lasing radiation, and Fresnel reflection. It should be noted that in our case, the losses due to the Fresnel reflection are dominant and amount to approximately 80% of the total losses. Specific losses in an active element, including scattering by defects and absorption at a wavelength of 1030 nm, are approximately 0.25 cm^{-1}. It should be noted that the losses of lasing radiation could be much smaller in the presence of antireflection coatings on the active element.

Table 5. Threshold pump power and lasing threshold amplification coefficient

Threshold pumping power, W	g_0, cm^{-1}	Reflectance output coupler
0.235 ± 0.007	1.11	0.995
0.304 ± 0.009	1.44	0.945
0.33 ± 0.099	1.56	0.900
0.411 ± 0.012	1.949	0.845

Conclusion

$Y_{2,55}Yb_{0,25}Sc_{1,00}Al_{4,2}O_{12}$ composition was selected from the area of existence of single-phase solid solutions based on yttrium-scandium-aluminum garnets doped with ytterbium. The lasing spectrum of the ceramics depended on the transmittance of the output mirror. A decrease in the transmittance led to a broadening of the lasing spectrum mainly in the long-wavelength area.

The maximum output power at the lasing wavelength in the quasi-continious wave pumping regime was 1.8 W at an absorbed pumping power of 3.6 W with a slope efficiency of 57%, which is a good indicator for an active element with uncoated edges. In the continuous wave pumping regime, the maximum power was 1.37 W with a slope efficiency of 41.7%. The results of the study show that this optical ceramics has a good optical quality and has good prospects to be used in laser systems operating in mode-locking regime

Funding

This paper was supported by a grant from the President of the Russian Federation MK-72.2022.1.2.

Conflict of interest

The authors declare that they have no conflict of interest.

References

[1] A. Ikesue, T. Kinoshita, K. Kamata , K. Yoshida. J. Am. Ceram. Soc., **78**(4), 1033–1040 (1995). DOI: 10.1111/j.1151-2916.1995.tb08433.x

[2] M. KučDera, P. Hasa, J. Hakenová. J. Alloys Compd., **451**, 146–148 (2008). DOI: 10.1002/pssr.201307256

[3] A. Ikesue, Y.L. Aung, J. Wang. Progress in Quantum Electronics, **100416**, 1–34 (2022). DOI: 10.1016/j.pquantelec.2022.100416
[4] A. Ikesue, T. Kinoshita, K. Kamata, K. Yoshida. J. Am. Ceram. Soc., **78**(4), 1033–40 (1995). DOI: 10.1111/j.1151-2916.1995.tb08433.x
[5] J. Lu, M. Prabhu, J. Song, C. Li, J. Xu, K. Ueda, A.A. Kaminskii, H. Yagi, T. Yanagitani. Appl. Phys. B., **71**, 469–473 (2000). DOI: 10.1007/s003400000394
[6] J. Saikawa, Y. Sato, T. Taira, A. Ikesue. Opt. Mater., **29**, 1283–1288 (2007). DOI: 10.1016/ j. optmat.2006.01.031
[7] Y. Sato, T. Taira, A. Ikesue. J. Appl. Phys., **42**, 5071–5074 (2003). DOI: 10.1143/JJAP.42.5071
[8] J. Dong, K. Ueda, A. Kaminskii. Opt. Express, **16**, 5241–5251 (2008). DOI: 10.1364/oe.16.005241
[9] F. Cornacchia, R. Simura, A. Toncelli, M. Tonelli, A. Yoshikawa , T. Fukuda. Opt. Mater., **30**, 135–138 (2007). DOI: 10.1016/j. optmat.2006.11.029
[10] A.R. Reinberg, L.A. Riseberg, R.M. Brown, R.W. Wacker, W.C. Holton. Appl. Phys. Lett., **19**, 11–13 (1971). DOI: 10.1063/1.1653721
[11] M.S. Nikova, I.S. Chikulina, A.A. Kravtsov, V.A. Tarala, F.F. Malyavin, E.A. Evtushenko, L.V. Tarala, D .S. Vakalov, D.S. Kuleshov, V.A. Lapin, E.V. Medyanik, V.S. Zyryanov. Nauchno-tekhnicheskiy vestnik informatsionnykh tekhnologiy, mekhaniki i optiki, **19**, 630 (2019) (in Russian). DOI: 10.17586/2226-1494-2019-19-4-630-640
[12] A.S. Protasov, M.O. Senina, D.O. Lemeshev. Uspekhi v himii i himicheskoj tekhnologii, **34** (5), 80 (2020). (in Russian)
[13] M.S. Nikova, V.A. Tarala, F.F. Malyavin, D.S. Vakalov et al Ceramics International, **47**, 1772–1784 (2021). DOI: 10.1016/j.ceramint.2020.09.003
[14] R.D. Shannon. Acta Crystallographica, **32**, Pages 751–767 (1976). DOI: 10.1107/S0567739476001551
[15] G.B. Lutts, A.L. Denisov, E.V. Zharikov, A.I. Zagumennyi, S.N. Kozlikin, S.V. Lavrishchev, S.A. Samoylova, Opt. Quantum Electron., **22**, 269–281 (1990). DOI: 10.1007/BF02089015
[16] Alban Ferrier, Simon Ilas, Philippe Goldner, Anne Louchet-Chauvet, J. Lumin., **194**, 116–122 (2018). DOI: 10.1016/j.jlumin.2017.09.056
[17] M.S. Nikova, V.A. Tarala, A.A. Kravtsov, I.S. Chikulina, D.S. Vakalov, L.V. Tarala, S.N. Kichuk, F.F. Malyavin, L.V. Kozhitov, S.V. Kuznetsov. Ceramics International, **48** (24), 36739–36747 (2022). DOI: 10.1016/j.ceramint.2022.08.235
[18] A.A. Kaminsky, L.K. Aminov, V.L. Ermolaev. *Fizika i spektroskopiya lazernykh kristallov* (Nauka, M., 1986). (in Russian)
[19] Jiro Saikawa, Yoichi Sato, Takunori Taira, Akio Ikesue. Optical Materials, **29** (10), 1283–1288 (2007). DOI: 10.1016/j.optmat.2006.01.031
[20] E.A. Radjabov, A.V. Samborsky. Izvestiya RAN. Ser. fiz. **81**, 1173 (2017) (in Russian).
[21] C. Xingtao, W. Yiquan, W. Nian, Q. Jianqi, L. Zhongwen, Z. Qinghua, H. Tengfei, Z. Qiang, L. Tiecheng. J. Eur. Ceram. Soc., **38**(4) 1957–1965 (2018). DOI: 10.1016/j.jeurceramsoc.2017.11.055
[22] Z. Lu, T. Lu, N. Wei, W. Zhang, B. Ma, J. Qi, Y. Guan, X. Chen, H. Wu, Y. Zhao. Optical Materials, **47**, 292–296 (2015). DOI: 10.1016/j.optmat.2015.05.043
[23] N. Jiang, C. Ouynag, Y. Liu, W. Li, Y. Fu, T. Xie and Q. Liu. Opt. Mater., **95**, 109203 (2019). DOI: 10.1016/j.optmat.2019.109203
[24] T. Kushida, E. Takushi, V. Oka., J. Lumin., **12**(13), 723–727 (1976).
[25] V.P. Lebedev, A.K. Przhevyskii. FTT, **19**, 1373–1376 (1977).
[26] M.S. Nikova, V.A. Tarala, F.F. Malyavin, D.S. Vakalov, V.A. Lapin, D.S. Kuleshov, A.A. Kravtsov, I.S. Chikulina, L.V. Tarala, E.A. Evtushenko, E.V. Medyanik, S.O. Krandievsky, A.V. Bogach, S.V. Kuznetsov, Ceramics International, **47** (2), 1772–1784 (2022). DOI: 10.1016/j.ceramint.2020.09.003
[27] T. Kushida, E. Takushi, V. Oka. J. Lumin., **12** (13). 723–727 (1976).
[28] V.P. Lebedev and A.K. Przhevuskii, FTT, **19**, 1373–1376 (1977). (in Russian).
[29] M. Pollnau, M. Eichhorn. In: *Nano-Optics: Principles Enabling Basic Research and Applications,* ed by B. Di Bartolo, J. Collins, L. Silvestri. NATO Science for Peace and Security Series B: Physics and Biophysics (Springer, Dordrecht, 2017), p. 387. DOI: 10.1007/978-94-024-0850-8_19
[30] G.A. Bogomolova, D.N. Vylegzhanin, A.A. Kaminski. Eksp. Teor. Fiz., **69**. 860–874 (1975).
[31] Jorg Korner, Mathias Kruger, Jurgen Reiter, Andreas Munzer, Joachim Hein, Opt. Soc. Am., **10**, 2425–2438 (2020). DOI: 10.1364/OME.398740
[32] Umit Demirbas, Jelto Thesinga, Martin Kellert, Mikhail Pergament, Franz X. Kärtner, Optical Materials, **112**, (2021). DOI: 10.1016/j.optmat.2020.110792.
[33] G. Toci, A. Pirri, B. Patrizi, Y. Feng, T. Xie, Z. Yang, J. Li, M. Vannini. Ceramics International, **46**, 17252–17260 (2020). DOI: 10.1016/j.ceramint.2020.04.012
[34] J. Saikawa, Y. Sato, T. Taira, A. Ikesue. Appl. Phys. Lett., **85**, 1898–1900 (2004). DOI:10.1063/1.1791339
[35] A. Pirri, G. Toci, J. Li, Y. Feng, T. Xie, Z. Yang, B. Patrizi, M. Vannini. Materials, **11**(5), 837–845 (2018). DOI: 10.3390/ma11050837
[36] Y. Feng, G. Toci, A. Pirri, B. Patrizi, Z. Hu, J. Wei, H. Pan, X. Zhang, X. Li, S. Su, M. Vannini, J. Li. J. Am. Ceram. Soc., **9**(5), 1–11 (2019). DOI: 10.1007/s40145-020-0403-8
[37] Y. Feng, G. Toci, A. Pirri, B. Patrizi, X. Chen, J. Wei, H. Pan, X. Zhang, X. Li, M. Vannini, J. Li. J. Alloys and Compounds, **815**, 152637 (2020). DOI: 10.1016/j.jallcom.2019.152637
[38] V. Kushawaha, A. Banerjee, L. Major. Appl. Phys. B., **56**, 239–242 (1993). DOI: 10.1007/BF00348632
[39] D. Findlay, R.A. Clay. Phys. Lett., 20, 277–278 (1966). DOI: 10.1016/0031-9163(66)90363-5
[40] Yaacob Mat Daud, Abd Rahman Tamuri, Noriah Bidin. J. Fiz. UTM, **3**, 38–42 (2008).

Translated by E.Potapova